



Hybrid Temperature-Reactivity PID Controllers for Nuclear Thermal Propulsion Startup

May 2023

Changing the World's Energy Future

Vincent M Laboure, Stefano Terlizzi, Sebastian Schunert



INL is a U.S. Department of Energy National Laboratory operated by Battelle Energy Alliance, LLC

DISCLAIMER

This information was prepared as an account of work sponsored by an agency of the U.S. Government. Neither the U.S. Government nor any agency thereof, nor any of their employees, makes any warranty, expressed or implied, or assumes any legal liability or responsibility for the accuracy, completeness, or usefulness, of any information, apparatus, product, or process disclosed, or represents that its use would not infringe privately owned rights. References herein to any specific commercial product, process, or service by trade name, trade mark, manufacturer, or otherwise, does not necessarily constitute or imply its endorsement, recommendation, or favoring by the U.S. Government or any agency thereof. The views and opinions of authors expressed herein do not necessarily state or reflect those of the U.S. Government or any agency thereof.

Hybrid Temperature-Reactivity PID Controllers for Nuclear Thermal Propulsion Startup

Vincent M Laboure, Stefano Terlizzi, Sebastian Schunert

May 2023

**Idaho National Laboratory
Idaho Falls, Idaho 83415**

<http://www.inl.gov>

**Prepared for the
U.S. Department of Energy
Under DOE Idaho Operations Office
Contract DE-AC07-05ID14517**

Hybrid Temperature-Reactivity PID Controllers for Nuclear Thermal Propulsion Startup

Vincent M. Labouré, Stefano Terlizzi, and Sebastian Schunert

*Reactor Physics Methods and Analysis Group, Idaho National Laboratory, 1955 N Fremont Ave, Idaho Falls, ID,
vincent.laboure@inl.gov*

In this work, a novel temperature-reactivity controller is introduced to rotate control drums based on a chamber temperature signal. It consists of two components: (1) a reactivity-driven proportional controller converting the temperature demand into a reactivity signal, and (2) a temperature-driven proportional-derivative controller which relies on a derivative term to anticipate sudden changes in demand and limit temperature overshoot. A weighting function is proposed to continuously transition from one component to the other.

I. INTRODUCTION

Given the very short duration over which nuclear thermal propulsion (NTP) systems must be able to reach nominal power, precisely following a chamber temperature demand—using control drums (CDs) as a means to control reactivity—is challenging to achieve without significant delay or overshoot. This is due to the inertia of the system, i.e., the intrinsic delay between the times at which the drums are rotated and the coolant temperature adjusts to the perturbation.

Previously, a standard proportional integral (PI) controller for temperature and pressure demands was used in Ref. [1], with delays and oscillations being observed after any sudden change in demand. With the controller gains adjusted as a function of total power, near-perfect agreement between the demands and the responses was obtained [2]. Simultaneously, a limited delay and little to no overshoot were obtained in Ref. [3] by converting the chamber temperature signal to a power signal to use in a period-generated controller (PGC) [4]. The disadvantage of this latter type of power-following (i.e., driven by a power signal) controller is that it requires to provide reactivity coefficients and the rates of change of the various temperatures affecting reactivity (e.g., fuel or moderator temperatures)—which need to be estimated in real-time.

A different type of power-following controller—a hybrid power-reactivity PI controller introduced in Ref. [5]—relied on the power and reactivity of the system to compute the CD angle without attempting to anticipate the future state of the system. Consequently, it did not require rates of change but showed similarly good performance as a PGC. Nevertheless, because it was only tested with a power signal, chamber temperature overshoots on the order of 7% were obtained on a prototypical startup sequence. The purpose of this work is to extend this type of controller by using chamber temperature, rather than power, as the demand while minimizing delay and overshoot. This is achieved by combining a proportional derivative (PD) controller with a temperature signal and a proportional (P) controller with a reactivity signal (approximately converted from the temperature signal). A sigmoid-like weighting is proposed to continuously transition from one controller to the other.

The resulting hybrid temperature-reactivity controller re-

lies solely on a temperature signal with fixed gains to actuate the CDs, without requiring reactivity coefficients and temperature rates of change. It is tested using a simplified multiphysics model with a point kinetics (PKE) neutronics model, and a single representative fuel assembly and fuel cooling channel. For this preliminary work, the mass flow rate and chamber pressure are assumed given and not controlled.

II. THEORY

In this section, the chamber temperature demand is denoted T_d whereas T is the actual chamber temperature of the system (measured or predicted, in the case of a real system or numerical model, respectively). An ideal controller is able to achieve $T = T_d$.

II.A. Controller with Direct Temperature Signal

A widely used approach is to convert the error, $\varepsilon(t) = T_d - T$, into a proportional integral derivative (PID) correction signal to actuate the drums:

$$\Delta\theta_T(t) = K_p\varepsilon(t) + K_i \int_0^t \varepsilon(t') dt' + K_d \frac{d\varepsilon}{dt}, \quad (1)$$

where K_p , K_i , and K_d are the gains, usually tuned to achieve the optimum performance. In this work, they are assumed constant throughout the simulation. In a nutshell, the proportional, integral and derivative terms respectively react to the current, past and future performance of the controller. Therefore, unless the gains are made time-dependent (as in Ref. [2]), a simple PI controller cannot perfectly anticipate any sudden change in demand. A derivative term adds anticipation and can also reduce overshoot but, in real systems, it can lead to instabilities due to instrumentation noise.

II.B. Controller with Temperature-Inferred Reactivity Signal

The physical delays between the times at which (1) the drums are rotated, (2) the power adjusts to the perturbation and (3) the coolant temperature reacts to this change in power limit the ability to quickly react to change in demand. Conversely, a CD rotation results in a virtually immediate change in reactivity, which was the motivation in Ref. [5] for introducing a reactivity informed signal to control the drums. The first step is to convert the temperature demand to a power demand, \mathcal{P}_d , which can be approximately done as follows [3]:

$$\mathcal{P}_d \approx \dot{m}(H_{\text{out}}(T_d) - H_{\text{tank}}), \quad (2)$$

where \dot{m} is the total mass flow rate of propellant, H_{tank} is the enthalpy in the storage tank and $H_{\text{out}}(T_d)$ is the enthalpy

corresponding to the temperature of the temperature demand. In Ref. [3], this power demand is directly used in a PGC controller. Alternatively, this can be further converted into a reactivity demand, ρ_d , as was done in Ref. [5]:

$$\rho_d = \frac{\Lambda}{\beta_{\text{eff}} \beta_{\text{eff}}} \left(\frac{d\mathcal{P}_d}{dt} - \sum_i \lambda_i C_i \right) + 1, \quad (3)$$

where Λ is the neutron mean generation time, β_{eff} is the effective delayed neutron fraction, and λ_i is the decay constant of the delayed neutron precursor group i with concentration C_i . Note that both $\beta_{\text{eff}}/\Lambda$ and C_i can be obtained experimentally [6].

The CD correction angle is then computed as:

$$\Delta\theta_p(t) = K'_p e(t) + K'_i \int_0^t e(t') dt' + K'_d \frac{de}{dt}, \quad (4)$$

where $e(t) = \rho_d - \rho$ is the error in reactivity and K'_p , K'_i , and K'_d are the proportional, integral, and derivative gains of the reactivity-driven PID controller, respectively. Typically, K'_p can be chosen as the inverse of the differential CD worth so parameter tuning is simpler than the controller with a direct temperature signal. This controller tends to have a better initial response but it is not guaranteed to converge to the desired temperature due to the two successive and approximate conversions from temperature to reactivity signal [5].

II.C. Hybrid Temperature-Reactivity Controller

A third approach to combine the previous two controllers to benefit from the fast response of the reactivity-driven correction term while relying on the temperature-driven signal when the power approaches its nominal value. The resulting controller is illustrated in Figure 1. The only demand is the chamber temperature. It is used directly by the temperature-driven component and indirectly by the reactivity-driven component after a conversion using Equations (2) and (3) is performed. The CD angle is computed by a weighted sum of both corrections terms:

$$\theta(t_{n+1}) = \theta_i + \sum_{k=1}^n \Delta\theta(t_k) = \theta_i + \sum_{k=1}^n (\xi \Delta\theta_T(t_k) + (1 - \xi) \Delta\theta_p(t_k)), \quad (5)$$

where θ_i is the initial CD angle and t_k is the time at the k -th time step.

Multiple weighting functions are possible. In Ref. [5], two weighting functions were proposed for the power whose analogs for the temperature would be:

$$\xi = \xi_{\text{lin}} \equiv \frac{T_d - T_i}{T_f - T_i}, \quad (6)$$

$$\xi = \xi_{\text{log}} \equiv \frac{\log\left(\frac{T_d}{T_i}\right)}{\log\left(\frac{T_f}{T_i}\right)}, \quad (7)$$

where T_i is the initial chamber temperature (e.g., at the beginning of the bootstrap phase) and T_f is the nominal temperature.

For a power-following controller, both weightings performed virtually identically because of the outstanding performance of both components of the hybrid power-reactivity controller [5]. Another difference is that power can vary by two orders of magnitude or more during bootstrap and thrust build-up phases whereas temperature varies by at most a factor of 10. In addition, it was found to be beneficial to adjust the weighting function to $T_b \equiv T_d(t_b)$ where t_b is the time at which bootstrap ends (and thrust build-up begins). Specifically, the idea is to continuously and monotonically transition from the reactivity driven component ($\xi(T_i) = 0$) to the temperature-driven one ($\xi(T_f) = 1$) with equal contribution at the end of bootstrap ($\xi(T_b) = 0.5$). This can be achieved by defining a sigmoid-like function with finite bounds:

$$\xi = \xi_s(T_d) = \begin{cases} 0 & , T_d < T_i \\ \frac{1}{1 + \left(\frac{2(T_b - T_i)}{T_d - T_i} - 1\right)^s} & , T_i \leq T_d < T_b \\ \frac{1}{1 + \left(\frac{2(T_f - T_b)}{T_d + (T_f - 2T_b)} - 1\right)^s} & , T_b \leq T_d < T_f \\ 1 & , T_d \geq T_f \end{cases} \quad (8)$$

where s is a positive integer controlling the steepness of the function. Figure 2 plots ξ_s as a function of the temperature demand for various values of s . Increasing the value of s results in a faster transition from the reactivity-driven to the temperature-driven component.

III. RESULTS AND ANALYSIS

To study the performance of the temperature-following controllers presented in the previous section, a condensed start-up sequence is considered and a simplified model is derived.

III.A. Prototypical Bootstrap and Thrust Build-up Phases

The purpose of the start-up sequence is to assess the performance of the controllers with a rapid increase in temperature with some sudden changes in demand. The core is assumed to have finished thermal conditioning and prototypical bootstrap and thrust build-up phases are modeled with a duration of 10 and 35 s (with the last 15 s at nominal specific impulse), respectively. Specifically, the temperature demand is chosen to be:

- $T_d(t = 0 \text{ s}) = 500 \text{ K}$
- $T_d(t = 10 \text{ s}) = 700 \text{ K}$
- $T_d(t \geq 30 \text{ s}) = 2700 \text{ K}$,

with a linear increase in between points. The chamber pressure demand—which is not the focus of this work—is assumed to be:

- $p_C(t = 0 \text{ s}) = 0.02 \times p_{C,\text{nom}}$
- $p_C(t = 10 \text{ s}) = 0.13 \times p_{C,\text{nom}}$
- $p_C(t = 30 \text{ s}) = 0.65 \times p_{C,\text{nom}}$
- $p_C(t \geq 45 \text{ s}) = p_{C,\text{nom}}$,

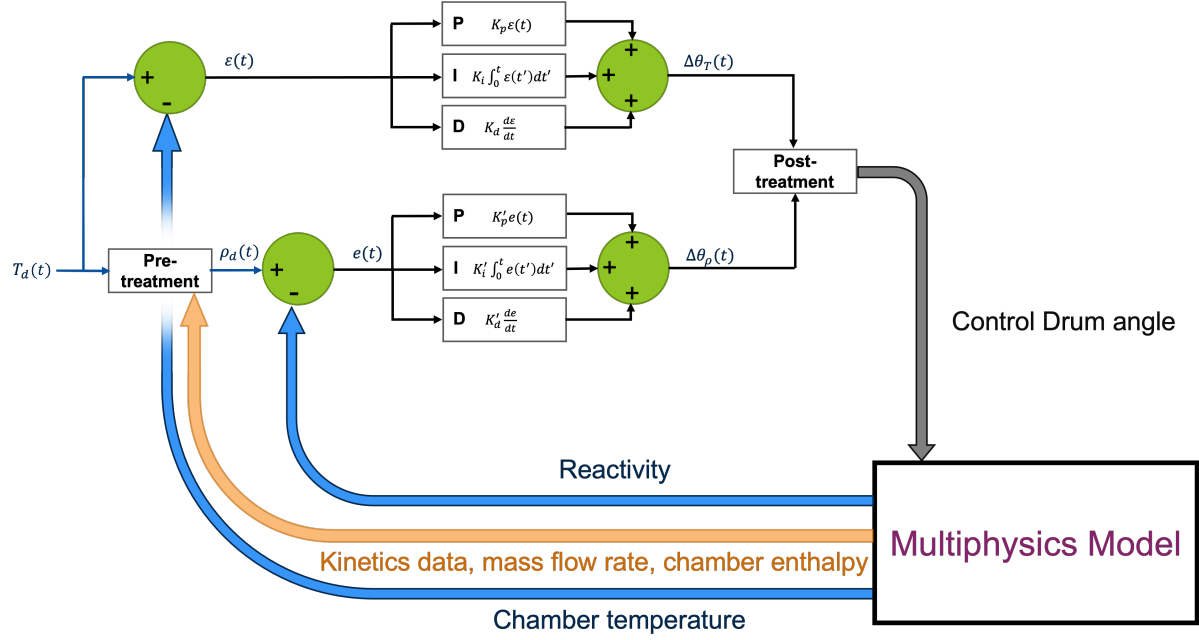


Fig. 1. Schematics of the hybrid temperature-reactivity controller.

with a linear increase in between points, where $p_{C,nom}$ is the nominal chamber pressure.

III.B. Simplified Model

The multiphysics model used for this study is greatly simplified compared to the one from [5] to reduce nonlinear effects and better understand the behavior of the controller itself. It remains based on the Multiphysics Object-Oriented Simulation Environment (MOOSE) framework [7]. In particular:

- The neutronics is modeled using a Griffin PKE model [8, 9], with constant CD reactivity worth (-25 pcm/deg), fuel temperature reactivity coefficient (-1 pcm/K) and kinetics parameters (summarized in Table I) and the initial reactor is assumed critical with 1 MW initial power. This implies that the initial state of the reactor is not a thermal equilibrium, which can be useful to test the robustness of the controllers presented in this work.
- A single representative 30-degree fuel assembly slice, shown in Figure 3 and extruded up at the height of the active core, is modeled with Bison [10]. All the power is assumed deposited in the fuel and with the only way for heat to be removed being by convection at the boundary of the fuel cooling channels (holes in Figure 3).
- A single representative fuel cooling mechanism preserving the main hydraulic parameters of the collection of all the fuel cooling channels (flow area, hydraulic diameter, etc.) is modeled with RELAP-7 [11] with an inlet coolant temperature of 300 K. The H_2 propellant is assumed to be an ideal gas with the specific heat capacity adjusted to match the expected enthalpy rise over a temperature range of 50–2700 K, as was done in Ref. [5].

The mass flow rate is assumed to be proportional to the chamber pressure. These significant simplifications will be improved in future work.

TABLE I. Kinetics parameters used in the neutronics model. λ_i and β_i are the delayed neutron decay constants and fractions, respectively. Λ is the mean generation time.

Delayed Group	λ_i (s ⁻¹)	β_i (pcm)	Λ (s)
1	1.3346×10^{-2}	24.6	1.33×10^{-5}
2	3.2667×10^{-2}	128.6	
3	1.2094×10^{-1}	124.3	
4	3.0444×10^{-1}	282.0	
5	8.5639×10^{-1}	121.7	
6	2.8764×10^0	50.8	
Sum		732.1	

III.C. Numerical Results

In the section a limited set of results is presented, exhibiting the potential benefits of using a hybrid temperature-reactivity controller. However, since all the controllers presented in the previous section are greatly affected by their gains, only the most relevant values tested are reported. However, a rigorous optimization has not been conducted at this point.

III.C.1. Controller with Direct Temperature Signal

If only the proportional term is considered, the proportional gain is set high enough to have a responsive system but low enough to avoid oscillations and overshoot. It is difficult

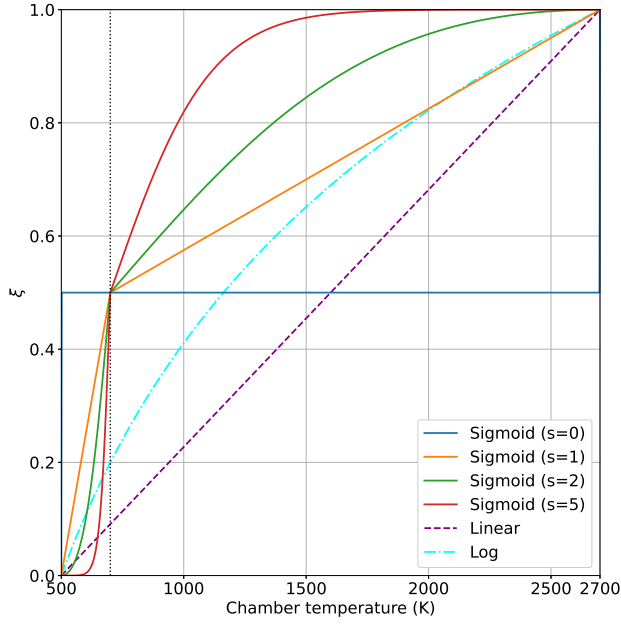


Fig. 2. Value of the weighting functions ξ for different options. The black vertical dotted line highlights the temperature at the end of the bootstrap phase (chosen to be $T_b = 700$ K).

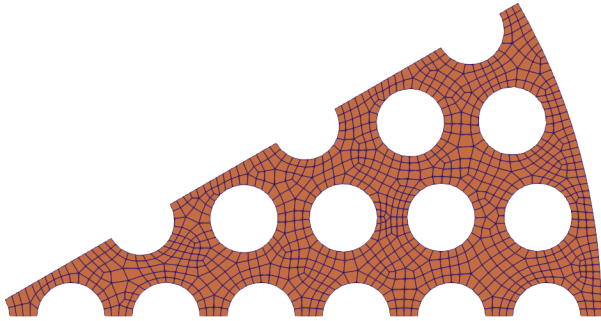


Fig. 3. X-Y view of the representative fuel assembly 30-degree slice used for the thermal model.

to achieve both requirements due to the inherent time delay between the time the CDs are rotated and the time the chamber temperature reacts to the perturbation. For instance, in Figure 4, the controller with $K_p = 5 \times 10^{-3}$ deg/K follows the trend of the demand reasonably well but the controller has an initial delay—partly due to the initial condition not being in thermal equilibrium—and a fairly oscillatory behavior with a temperature overshoot (defined as $(\max(T) - T_i)/(T_f - T_i)$) of 1.2%. Further increasing the gain would increase oscillations and overshoot whereas the opposite would further delay the initial response.

An integral term is found to lead to increased overshoot and is therefore not considered in this work. Note however that this is likely due to using constant gains as opposed to what was done in Ref. [2].

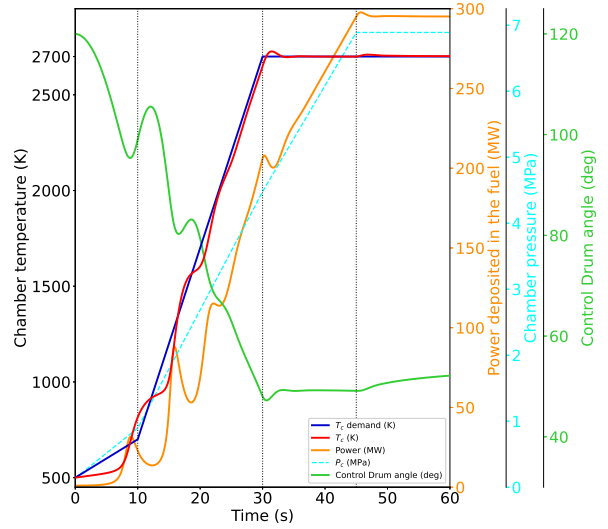


Fig. 4. Temperature proportional controller with a gain of $K_p = 5 \times 10^{-3}$ deg/K.

Figure 5 shows the results obtained with a temperature-driven PD controller ($K_p = 5 \times 10^{-3}$ deg/K, $K_d = 5 \times 10^{-3}$ deg-s/K). The derivative term helps anticipate sudden changes in demand and, despite some initial delay and oscillations during the bootstrap phase, the controller's behavior is quite satisfying for most of the thrust build-up phase. Compared to the case without derivative term, the temperature overshoot is reduced to 0.3% and occurs shortly after the chamber pressure demand (i.e., mass flow rate) reaches its nominal value. The initial delay, however, is virtually unchanged.

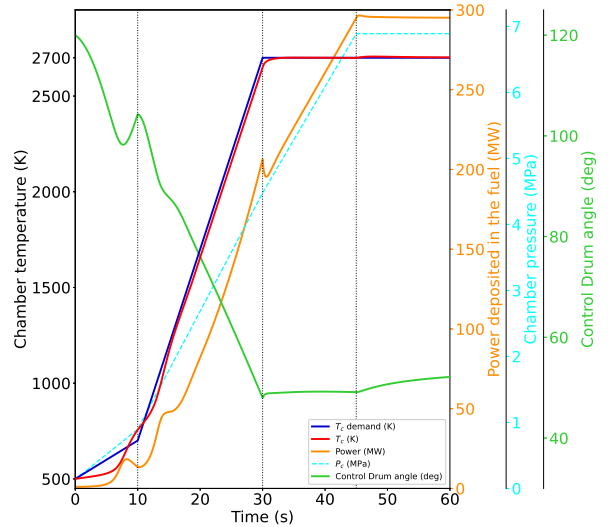


Fig. 5. Temperature PD controller with gains of $K_p = 5 \times 10^{-3}$ deg/K and $K_d = 5 \times 10^{-3}$ deg-s/K.

III.C.2. Controller with Temperature-Inferred Reactivity Signal

The advantage of a reactivity-driven controller is that it can determine, given a temperature demand, the required reactivity to achieve the desired ramp and a CD rotation can be done to immediately insert that amount of reactivity. Therefore, its initial response could be superior to a controller directly using a temperature signal. Figure 6 shows the results obtained using a proportional controller with the gain set to the inverse of the CD differential worth, i.e., $K'_p \approx 29.3$ deg/\$. The initial response of the controller is indeed improved. Nevertheless, such a controller is unable to ensure that the chamber temperature converges to the nominal demand since a zero error in reactivity does not necessarily imply the same for temperature. In fact, the coolant enthalpy rise shown in Figure 6 noticeably trails behind the actual power deposited in the fuel during the thrust build-up phase which indicates that the approximation done to convert the temperature demand into a power demand (see Equation (2)) is inaccurate during that time. As a result, the reactivity signal works on the assumption that the power matches the enthalpy rise but since the former is underestimated, the final power and chamber temperature stabilize about 10% higher than their desired values.

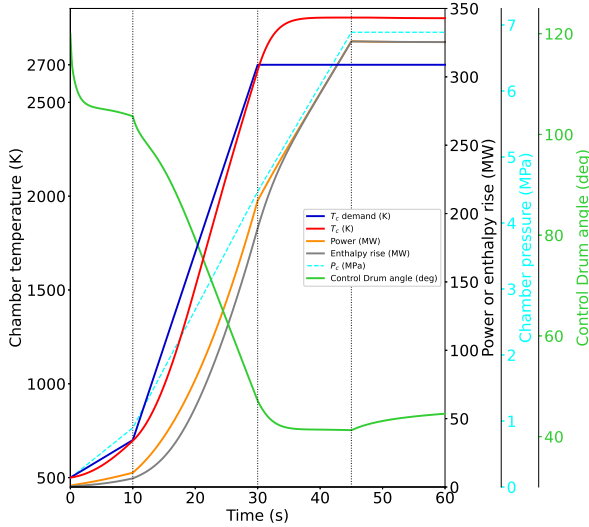


Fig. 6. Reactivity proportional controller with a gain of $K'_p \approx 29.3$ deg/\$.

III.C.3. Hybrid Temperature-Reactivity Controller

The core idea of this work is to use the reactivity-driven controller at early stages and then continuously transition to the temperature PD controller. The sigmoid-like weighting function with $s = 5$ (see Figure 2) is used to operate the transition quickly. Figure 7 gives the corresponding results. As expected, the initial response of the controller is better than using the temperature PD controller and the chamber temperature stabilizes to the desired value of 2700 K with the same overshoot of 0.3% as temperature PD controller. A slightly larger delay is observed around the transition between the

bootstrap and thrust build-up phases which could be further alleviated by fine tuning of the controller's gains and of the expression of the weighting function.

IV. CONCLUSIONS

In this work, a hybrid temperature-reactivity controller was proposed. It consists of two components: (1) a reactivity-driven proportional controller converting the temperature demand into a reactivity signal with a decent initial response, and (2) temperature-driven PD controller which relies on a derivative term to anticipate sudden changes in demand and limit temperature overshoot. The novel controller here introduced, uses constant gains, thereby simplifying the tedious process of gain tuning, and does not rely on reactivity coefficients and the rates of change, that could be difficult to estimate in real-time, as for the PGC controller. Despite having several positive characteristics, one of its main disadvantages is that derivative signals are subject to noise in real systems so the instrumentation signal would need to be filtered appropriately to limit instability. Future work will investigate the effect of noise on the controller's performance and the deployment of this novel controller on a more elaborate multiphysics model, such as the one considered in Ref. [5]. Finally, the control logic will be extended to incorporate a chamber pressure controller. In addition, the reactivity will be controlled through both control drums and structural support control valves.

V. ACKNOWLEDGMENTS

This manuscript was authored by Battelle Energy Alliance, LLC under contract no. DE-AC07-05ID14517 with the U.S. Department of Energy. The U.S. Government retains and the publisher, by accepting the article for publication, acknowledges that the U.S. Government retains a nonexclusive, paid-up, irrevocable, worldwide license to publish or reproduce the published form of this manuscript, or allow others to do so, for U.S. Government purposes.

This research made use of the resources of the High Performance Computing Center at Idaho National Laboratory, which is supported by the Office of Nuclear Energy of the U.S. Department of Energy and the Nuclear Science User Facilities under contract no. DE-AC07-05ID14517.

REFERENCES

1. C. R. JOYNER, T. JENNINGS, D. E. HANKS, and D. J. LEVACK, "NTP Engine System Design and Modeling," in "ASCEND 2022," Las Vegas, Nevada & Online (October 24-26 2022).
2. T. JENNINGS, "Latest NTP Engine System Design and Modeling Results," (personal communication, January 2023).
3. V. MANICKAM, M. KRECICKI, and D. KOTLYAR, "Methodology and Preliminary Results for the Transient Control of Pressure and Temperature for Nuclear Thermal Propulsion Engines," in "International Conference on Physics of Reactors 2022 (PHYSOR 2022)," Pittsburgh, PA, USA (May 15-20 2022).

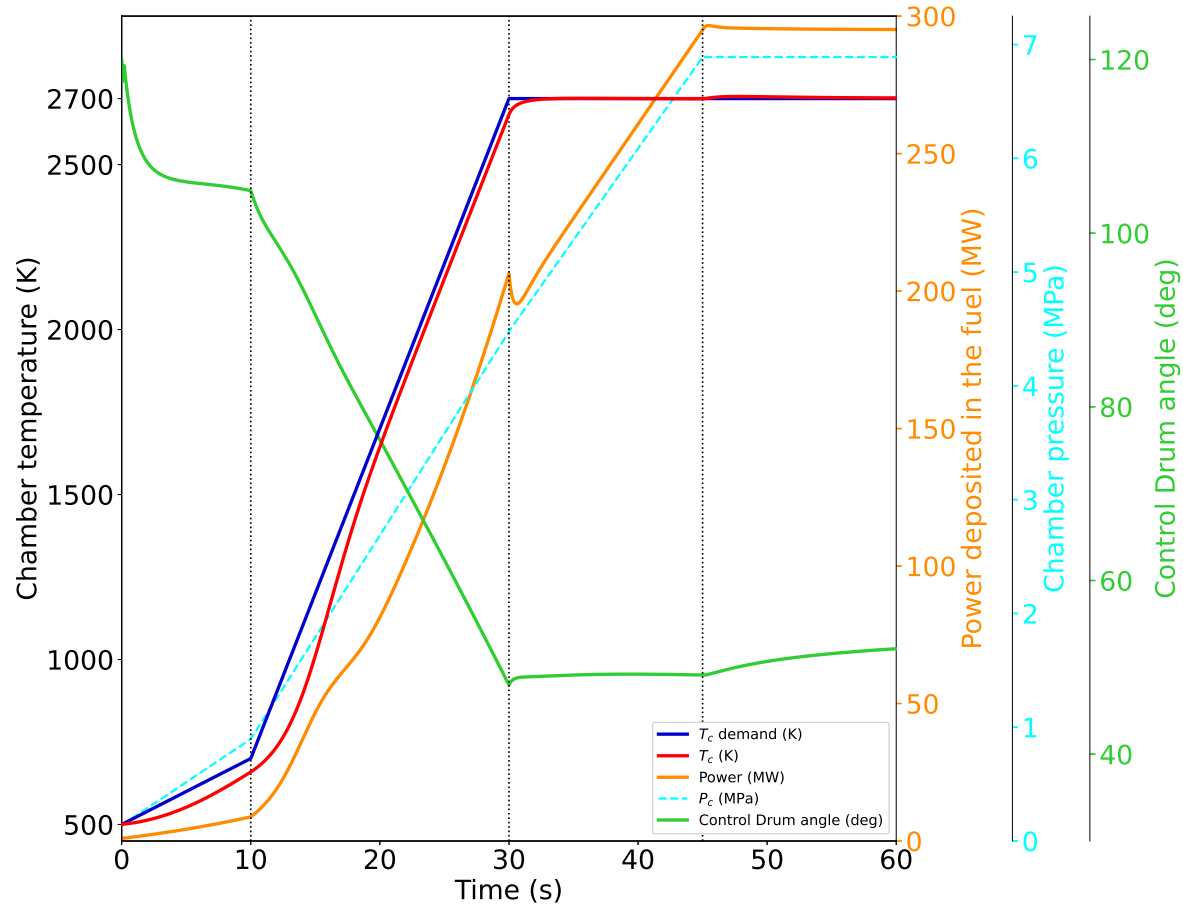


Fig. 7. Hybrid temperature-reactivity controller with gains of $K_p = 5 \times 10^{-3}$ deg/K, $K_d = 5 \times 10^{-3}$ deg-s/K, and $K'_p \approx 29.3$ deg/\$ using Equation (8) with $s = 5$ for the weighting.

4. J. A. BERNARD and D. D. LANNING, "Considerations in the Design and Implementation of Control Laws for the Digital Operation of Research Reactors," *Nuclear Science and Engineering*, **110**, 425–444 (1992).
5. V. M. LABOURÉ, S. SCHUNERT, S. TERLIZZI, Z. M. PRINCE, J. ORTENS, C.-S. LIN, L. C. M. CHARLOT, and M. D. DEHART, "Automated Power-following Control for Nuclear Thermal Propulsion Startup and Shutdown Using MOOSE-based Applications," *submitted to Progress in Nuclear Energy* (January 2023).
6. ÖZER CIFTCIOGLU and M. GECKINLI, "A CAMAC-based reactivity-meter for nuclear reactors," *Nuclear Instruments and Methods*, **177**, 2, 321–326 (1980).
7. C. J. PERMANN, D. R. GASTON, D. ANDRS, R. W. CARLSEN, F. KONG, A. D. LINDSAY, J. M. MILLER, J. W. PETERSON, A. E. SLAUGHTER, R. H. STOGNER, and R. C. MARTINEAU, "MOOSE: Enabling massively parallel multiphysics simulation," *SoftwareX*, **11**, 100430 (2020).
8. Y. WANG, S. SCHUNERT, J. ORTENS, V. M. LABOURÉ, M. D. DEHART, Z. M. PRINCE, F. KONG, J. R. HARTER, P. BALESTRA, and F. N. GLEICHER, "Rattlesnake: A MOOSE-Based Multiphysics Multi-scheme Radiation Transport Application," *Nuclear Technology*, **207**, 7, 1047–1072 (2021).
9. Y. JUNG and C. LEE, "PROTEUS-MOC User Manual," Tech. Rep. ANL/NE-18/10, Argonne National Laboratory (2018).
10. R. L. WILLIAMSON, J. D. HALES, S. R. NOVASCONE, G. PASTORE, K. A. GAMBLE, B. W. SPENCER, W. JIANG, S. A. PITTS, A. CASAGRANDA, D. SCHWEN, A. X. ZABRISKIE, A. TOPTAN, R. GARDNER, C. MATTHEWS, W. F. LIU, and H. L. CHEN, "BISON: A Flexible Code for Advanced Simulation of the Performance of Multiple Nuclear Fuel Forms," *Nuclear Technology*, pp. 1–27 (2021).
11. R. A. BERRY, J. W. PETERSON, H. ZHANG, R. C. MARTINEAU, H. ZHAO, L. ZOU, and D. ANDRS, *RELAP-7 Theory Manual*, INL (2014).